Auger spectra and band structure of $La_{1.85}Sr_{0.15}CuO_4$ and $La_{1.85}Ba_{0.15}CuO_4$

R. Bar-Deroma and J. Felsteiner
Department of Physics, Technion–Israel Institute of Technology, 32000 Haifa, Israel

R. Brener
Solid State Institute, Technion–Israel Institute of Technology, 32000 Haifa, Israel

J. Ashkenazi
Department of Physics, University of Miami, Coral Gables, Florida 33124

D. van der Marel
Department of Applied Physics, Delft University of Technology, 2628 CJ Delft, The Netherlands
(Received 14 February 1991; revised manuscript received 12 August 1991)

High-resolution Auger electron spectra of $La_{1.85}Sr_{0.15}CuO_4$ and $La_{1.85}Ba_{0.15}CuO_4$ have been measured. The experimental Auger line shapes of the oxygen KLL and copper $L_{2,3}VV$ transitions are compared with those generated from local-density-approximation linear-muffin-tin-orbital band-structure calculations. An analysis based on this comparison is used to determine the Coulomb parameters U_p and U_d of the oxygen and copper atoms, respectively. For this purpose, an extended version of Cini and Sawatzky's expression for the theoretical Auger line shape is used, taking into account the multiplet structure of the Auger final states and the point symmetry of the oxygen sites. We find U_p of approximately 5 and 7 eV for the planar and apical oxygen sites, respectively, and U_d of 7–8 eV for copper. An estimate of the effect of electron correlations on the band structure suggests a decrease of the anisotropy found in U_p.

I. INTRODUCTION

One of the basic problems in high-T_c superconductivity is the role of electron correlations. Their importance is, roughly, determined by the ratio between the relevant intra-atomic Coulomb integral U and the bandwidth. Already early in 1987, theoretical works on high-T_c cuprates have been split between the large-U theories[1] of highly correlated electrons, and small-U-limit works where the local-density approximation (LDA) has been applied to calculate the electronic structure.[2]

There exists a variety of experimental and theoretical results[3,4] supporting the important role of electron correlations, and quite large values of U have been evaluated on the basis of first-principles calculations.[5,6] There has been a controversy concerning the reliability of LDA band-structure results in these materials. Photoemission measurements on low-temperature cleaved single crystals of high-T_c cuprates[7] show that LDA calculations predict the Fermi surface correctly, however, experimentally the effective mass is found to be renormalized and the spectra have an anomalous energy dependence, consistent with rather opposing views based on correlated electrons[8] (see also Ref. 4). Also an anomalously strong background in the photoemission spectra has been found, as well as d^8 satellites at high binding energies.[9] In order to provide a further test of the applicability of the LDA band-structure calculation to this type of strongly correlated material we present in this paper linear-muffin-tin-orbital (LMTO) calculations in combination with theoretical expressions for the Auger line shape and compare these with Auger electron spectroscopy (AES) measurements of the two-hole excitations in the valence band.

AES is unique as an experimental tool concerning estimates of U since the Auger line shape reflects a two-hole density of states (DOS).[10] There are some reported AES measurements[11] for the $La_{2-x}Sr_xCuO_4$ and $La_{2-x}Ba_xCuO_4$ (La-Cu-O group) compounds but no information about the Cu($3d$) and O($2p$) Coulomb parameters is given. Such information has, however, been given for $YBa_2Cu_3O_7$ (Y-Ba-Cu-O).[12,13] In this work we report the values of the Cu($3d$) and the O($2p$) Coulomb parameters for the La-Cu-O group obtained from Auger electron line-shape measurements of the oxygen KLL and copper $L_{2,3}VV$ transitions. The Coulomb parameters are estimated using an extended version of Cini and Sawatzky's expression for the theoretical Auger line shape,[14] taking into account the multiplet structure of the Auger final states and the point symmetry of the oxygen sites.

II. COMPUTATIONS

The computational work involves LDA calculations of the partial density of states (PDOS) by the LMTO band-structure method.[15] The virtual-lattice approximation enabled us to take into account the Sr and Ba for noninteger x. Within the framework of the LMTO method this was done by taking a weighted average of the LMTO potential parameters of the alloy constituents according to their atomic percentage. The calculations were carried out on the body-centered tetragonal phase (space group $I4/mmm$) of $La_{1.85}Sr_{0.15}CuO_4$ and $La_{1.85}Ba_{0.15}CuO_4$. We

used the low-temperature values of the lattice parameters determined by Jorgensen *et al.*[16] The exact structure of the superconductors of the La-Cu-O type is orthorhombic and contains two formula units per unit cell, but its deviation from the tetragonal structure we used for the calculations is very small.

Within the framework of the atomic sphere approximation to the LMTO method,[15] the crystal volume is covered by overlapping spheres centered at each atomic site. The sum of their volumes equals the crystal volume, and inside each of them the potential is spherically symmetric. The error introduced by such a space-violating construction is largely compensated by the "combined corrections."[15] In order to get an optimal space coverage, we have added in each unit cell two "empty spheres" (ES), i.e., containing no nuclei. Their positions were fixed according to the crystal symmetry at $(\frac{1}{2},0,\frac{1}{4})$ and $(-\frac{1}{2},0,-\frac{1}{4})$. During the calculations, the radii of the spheres were modified in order to fulfill two other conditions: that the partial atomic pressures be close to zero, for the experimental atomic positions, and that the total charge within each sphere be close to zero. In this way, an optimal convergence of the LMTO method is obtained. The values of the converged sphere radii are presented in Table I. Muffin-tin orbitals[15] with angular momenta $l \leq 3$ for the La site, $l \leq 2$ for the Cu site, and $l \leq 1$ for the O(1), O(2), and ES sites were used [O(1) represents the oxygen atoms in the CuO_2 planes and O(2) the apical oxygen atoms outside these planes].

The Auger line shape was calculated using two degrees of sophistication. One approximation was to use the Cini-Sawatzky expression[14] for the two-hole local DOS in a completely filled, nondegenerate tight-binding band:

$$A(E)=\frac{N(E)}{[1-UH(E)]^2+[\pi UN(E)]^2}, \quad (1)$$

where $N(E)$ is the self-convolution of the single-hole PDOS and $H(E)$ is the Hilbert transform of $N(E)$. For unfilled bands, the full-band expression can still be used as an approximation,[17] provided that the number of holes per valence state is much smaller than 1 and that U is not too large.

We will assume that this is still correct for the oxygen atoms, as the O^{2-} ions have a closed-shell configuration. The deviations from the p^6 configuration in the ground state due to hybridization and hole doping are then treated by truncating the density of states obtained from the LMTO calculations at E_F. The situation is different for the Cu($3d$) states, as the Cu^{2+} ion has an open d shell with 9 d electrons. This fact, together with the O(p)-Cu(d) hybridization, is responsible for the presence of satellites in the valence and core-level photoelectron spectra of the copper-related states. For the Auger spectra this also results in a splitting of all spectral features in a main line and satellites. In order to get an order of magnitude estimate of U on the copper sites, we will nevertheless make a comparison between calculated spectra based on the Cini-Sawatzky expression and the measured spectra. As there is no physical reason why the spectral features can be reproduced correctly with this simplified approach, we do not attempt to treat the multiplet splitting of the Auger final states for the copper Auger spectrum. For pure copper oxides, Hartree-Fock cluster calculations have been carried out by Eskes and coworkers[18] to obtain the core-level and Auger electron line shapes.

TABLE I. Atomic spheres radii, in units of Å, used for $La_{1.85}Sr_{0.15}CuO_4$ and $La_{1.85}Ba_{0.15}CuO_4$. ES denotes empty spheres.

	$La_{1.85}Sr_{0.15}CuO_4$	$La_{1.85}Ba_{0.15}CuO_4$
R(La)	1.688	1.688
R(Sr)	1.688	
R(Ba)		1.982
R(Cu)	1.107	1.107
R(O(2))	0.905	0.905
R(O(1))	1.227	1.104
R(ES)	1.479	1.479

A generalized version of the Cini-Sawatzky expression, taking into account the point symmetry of the O($2p$) levels and the full multiplet structure of the p^4 final states, was used to calculate the Auger line shape of the oxygen $KL_{2,3}L_{2,3}$ Auger line. This more complete analysis of the line shape is required in order to determine the two different values of U on the oxygen atoms O(1) and O(2). A similar approach has been used to study the LVV Auger spectra of transition-metal impurities.[19] The implementation of this formalism for the oxygen p shell on a site with orthorhombic point symmetry is described in the Appendix.

III. EXPERIMENTAL

The Auger electron high-resolution spectra were measured using a computerized Perkin-Elmer, PHI model 590A scanning Auger spectrometer. The Auger spectrometer included a coaxial electron gun and a single-pass cylindrical mirror analyzer operated with 0.3% resolution. Typical base pressure in the UHV chamber was 5×10^{-10} Torr. The single-phase polycrystalline pellets studied here were prepared by a standard procedure of melting high-purity binary oxide powders. The samples were examined by using x-ray powder diffraction and T_c measurements. The samples were cleaned *in situ* by scraping with a diamond grinder. The cleaning procedure was repeated periodically so that Auger signals of the contaminants were kept below the AES detectability limits.

High-energy-resolution Auger line shapes were recorded with a 3-keV, 0.5-μA rastered primary electron beam in the first derivative mode, using 1 eV modulation voltage. The calibration of the kinetic energy scale relative to the vacuum level was performed by measuring the positions of the Auger electron peaks of the sputter-cleaned Ag and Cu metals. The "true" Auger line shapes were obtained after integration and appropriate background subtraction.[20] The inelastic-scattering contribution was removed by deconvoluting[21] an electron backscatter spectrum taken at the same kinetic energy as the Auger transition under study. The spectra were measured for the

transitions $L_{2,3}VV$ of copper and KVV of oxygen. For the purpose of comparison and interpretation of the results, we have also carried out measurements on bulk Y-Ba-Cu-O.

IV. RESULTS AND INTERPRETATION

The band-structure calculation converged using the tetrahedral interpolation scheme[15] with 45 **k** points in an irreducible part of the Brillouin zone. For the final DOS curves 273 **k** points were used. The error bars on the band energies, due to the approximation involved in our LMTO calculation (within the LDA) are estimated to be around 40–50 mRy (0.5–0.7 eV). Estimates of the error in the DOS due to the LDA are harder to make, and can be deduced from comparison with experiment (see below).

In Figs. 1 and 2 we present the energy band structure obtained for $La_{1.85}Sr_{0.15}CuO_4$ and $La_{1.85}Ba_{0.15}CuO_4$ along symmetry lines in the Brillouin zone. There have been band-structure calculations[2,22–26] of $La_{2-x}M_xCuO_4$ (M = Sr or Ba) for $0<x<1$. Most of the calculations were done for $x=0,1$ or a supercell including a number of formula units has been taken. In this work we have treated arbitrary x values by the virtual-lattice approximation, as explained above.

In Figs. 3 and 4 we show the total DOS and the PDOS for each atom in $La_{1.85}Sr_{0.15}CuO_4$ and $La_{1.85}Ba_{0.15}CuO_4$, respectively, in units of states/[eV×(unit cell)]. We must note that for the copper and oxygen atoms these PDOS's represent to a good approximation the Cu($3d$) band for the copper and the O($2p$) band for the oxygen. In general we can see the same structure for the two compounds. Above E_F there are the $5d$ and $4f$ bands of lanthanum. As in other LDA calculations for the cuprate superconductors, the states near E_F belong mainly to the antibonding σ band of the Cu($d_{x^2-y^2}$)-O(p_x,p_y) orbitals (of the CuO_2 planes), but also the Cu(d_{z^2}) orbital contributes quite close to E_F. In our work the $5p$ states of lanthanum and the $2s$ states of oxygen were taken as core states. In some other works[23] these states were included in the variational calculations using another energy window.[15]

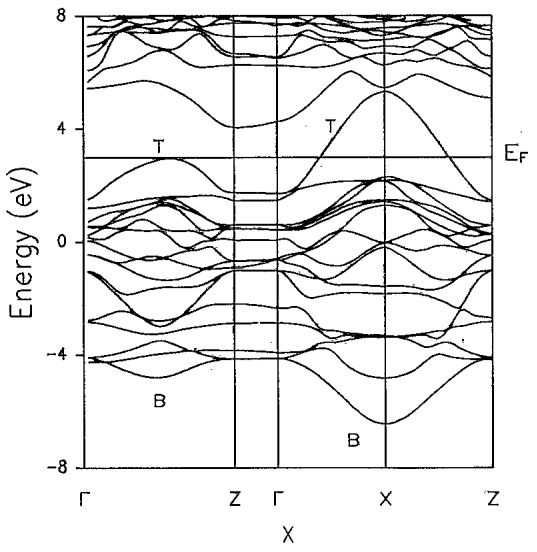

FIG. 1. Energy band structure for $La_{1.85}Sr_{0.15}CuO_4$.

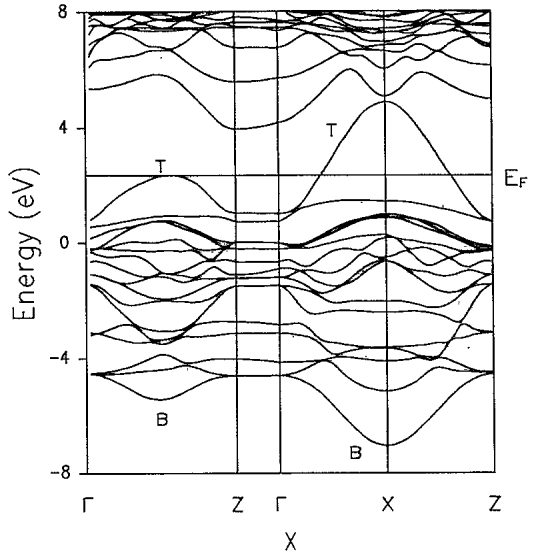

FIG. 2. Energy band structure for $La_{1.85}Ba_{0.15}CuO_4$.

Clearly there exists a difference between the structures of the PDOS's for the two oxygen sites O(1) and O(2); this will be discussed when the Auger spectra are analyzed below. In Table II, we present the values of the DOS at

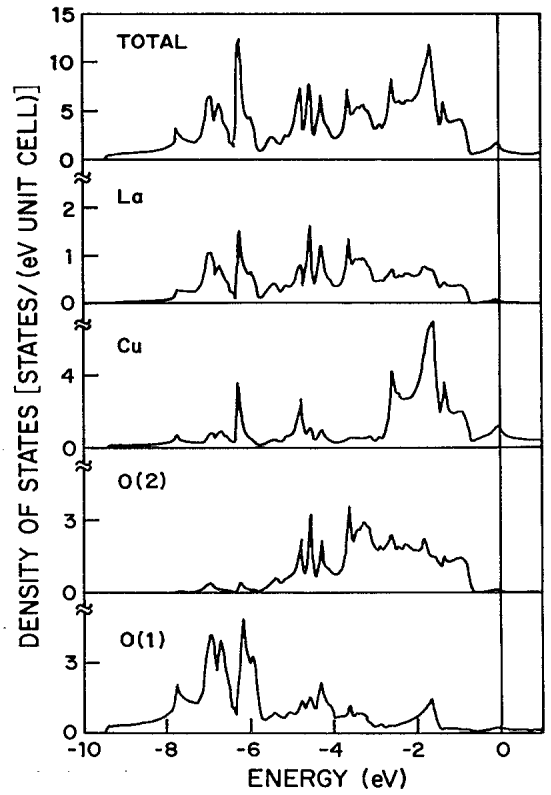

FIG. 3. Total and partial density of states for $La_{1.85}Sr_{0.15}CuO_4$. O(1) denotes the oxygen atoms in the CuO_2 planes and O(2) denotes the oxygen atoms outside the planes.

TABLE II. Density of states (DOS) in units of states/[Ry×(unit cell)] at the Fermi energy and the number of valence electrons (NOS) in the muffin-tin spheres for $La_{1.85}Sr_{0.15}CuO_4$ and $La_{1.85}Ba_{0.15}CuO_4$. ES denotes empty spheres.

		$La_{1.85}Sr_{0.15}CuO_4$		$La_{1.85}Ba_{0.15}CuO_4$	
		DOS	NOS	DOS	NOS
La	*s*	0.04	0.34	0.04	0.37
	p	0.09	0.53	0.11	0.58
	d	0.31	2.08	0.40	2.04
	f	0.28	1.11	0.39	1.07
Cu	*s*	0.67	0.32	0.79	0.36
	p	0.18	0.35	0.19	0.38
	d	11.21	9.33	10.76	9.34
O(2)	*s*	0.02	0.03	0.01	0.02
	p	1.34	7.88	2.08	8.49
O(1)	*s*	0.56	0.08	0.42	0.06
	p	2.66	9.90	2.70	9.45
ES	*s*	0.01	0.09	0.00	0.00
	p	0.08	0.79	0.10	0.67

the Fermi level in units of states/[Ry×(unit cell)] and the number of valence electrons in the atomic spheres for the two compounds. By comparison with other works, we find systematic differences in the bandwidth. In full-potential linear augmented plane waves (FLAPW) calculations the bandwidth is around 8 eV,[2,24] while in the LMTO calculations the bandwidth is about 9.5 eV,[23,25] which is closer to our results.

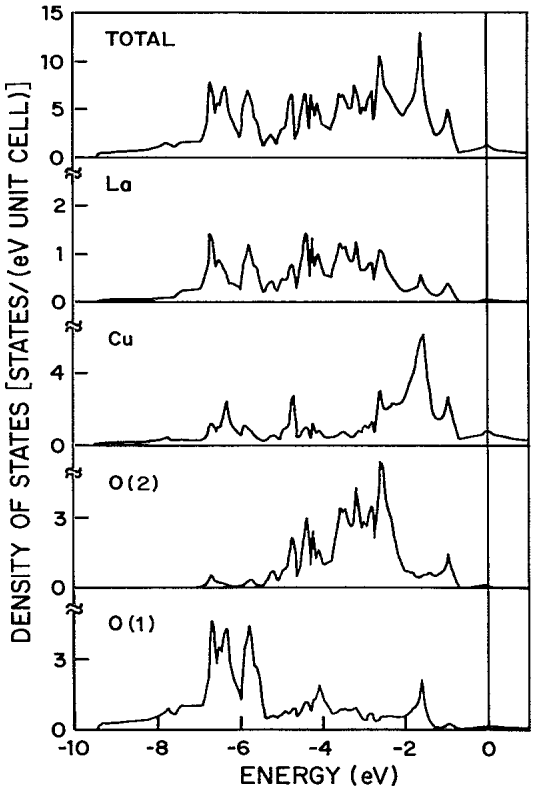

FIG. 4. Total and partial density of states for $La_{1.85}Ba_{0.15}CuO_4$. O(1) denotes the oxygen atoms in the CuO_2 planes and O(2) denotes the oxygen atoms outside the planes.

Our DOS results can be compared with experimental photoemission results.[27,28] Such comparison reveals shifts of 1–2 eV of the experimental peaks relative to ones calculated by us and other groups, including the FLAPW results.[24] A similar discrepancy in Y-Ba-Cu-O-type high-T_c superconductors has been proven to be largely a surface effect (due to the tendency of these compounds to lose oxygen),[7] and by doing the measurements on single crystals cleaved at $T=20$ K, good agreement has been obtained between the experimental and theoretical peaks, except for a range of ~ 1 below E_F. We do not know about similar measurements on superconductors of the La-Cu-O group.

In Fig. 5 we present the measured $L_{2,3}VV$ spectra of Cu in $La_{1.85}Sr_{0.15}CuO_4$, $La_{1.85}Ba_{0.15}CuO_4$, and $YBa_2Cu_3O_7$. These spectra consist of two lines corresponding to the L_3VV and L_2VV transitions. We cannot see any significant differences between the spectra for the three compounds. An asymmetry in the spectra can be seen in the low-energy side at a distance of 5.5–7 eV from the main line. This asymmetry is due to multiplet splitting in ^1G, ^3P, ^1S, and ^3F d^8 final states and additional multiplets corresponding to the d^7 final-state satellite lines.[12] Note that in the oxygen Auger it is not necessary to consider satellites corresponding to a p^3 final-state multiplet.

In Fig. 6 we present the Auger spectra of oxygen for $La_{1.85}Sr_{0.15}CuO_4$, $La_{1.85}Ba_{0.15}CuO_4$, and $YBa_2Cu_3O_7$. It is possible to distinguish four lines corresponding to the KL_1L_1, $KL_1L_{2,3}$ (^1P and ^3P), and $KL_{2,3}L_{2,3}$ transitions in oxygen. There is a fifth line (which does not appear in the $YBa_2Cu_3O_7$ spectrum) that corresponds to *MNN* transition in lanthanum. This peak was subtracted.

In Table III we present the energy position of the different transitions in the Auger spectra using two ener-

TABLE III. Experimental Auger energy peak positions (E_{kin} is in the kinetic-energy scale relative to the Fermi energy, and E_A is in the two-hole binding energy scale) and XPS core-level binding energies.

	$La_{1.85}Sr_{0.15}CuO_4$		$La_{1.85}Ba_{0.15}CuO_4$		$YBa_2Cu_3O_7$	
	E_{kin} (eV)	E_A (eV)	E_{kin} (eV)	E_A (eV)	E_{kin} (eV)	E_A (eV)
Cu(L_3VV)	917.2	16.3	917.3	16.0	916.7	16.1
Cu(L_2VV)	937.2	15.8	937.0	16.0	936.3	16.7
O($KL_{2,3}L_{2,3}$)	513.5	15.0	514.4	14.1	513.6	15.3
O(KL_1L_1)	477.2	51.7	477.6	51.3	478.0	50.9
			Binding energies (eV)			
Cu $E(L_2)$	953.0[a]		953.0[a]		953.0[b]	
Cu $E(L_3)$	933.5[c]		933.3[a]		932.8[b]	
O $E(K)$	528.5[c]		528.5[c]		528.9[b]	

[a]Liang *et al.*, Ref. 27.
[b]Balzarotti *et al.*, Ref. 13.
[c]Nücker *et al.*, Ref. 27.

gy scales, the kinetic energy scale and two-hole binding energy scale. We also present here the relevant core-level binding energies as measured by x-ray photoelectron spectroscopy (XPS), which define the threshold energy of the Auger spectra according to the rule $E_{kin}(\text{Auger}) = E_c(\text{XPS}) - E$, where E is the excitation energy of two (correlated) holes that appears in Eq. (1), and E_c(XPS) is the initial-state energy of the Auger process. There are several works where the Auger electron spectra of the Y-Ba-Cu-O and La-Cu-O groups were measured,[13,28] but most of them discussed the Auger lines of copper. Comparison between these published results and our results indicates a good agreement.

The theoretical Auger electron line shape was calculated using Eq. (1) for the copper $L_{2,3}VV$ Auger and expression (A4) of the Appendix for the oxygen KLL Auger. $N(E)$ in this expression represents the self-convolution of the PDOS for each atom. Thus, for copper we used the PDOS of the $3d$ band and for oxygen the PDOS of the $2p$ band. A comparison between the calculated and experimental Auger line shapes is used to get the value of U that appears as a parameter in Eq. (1). The calculated line shape was convoluted with a Gaussian in order to take into account the instrumental broadening and the broadening due to the lifetime of the holes during the Auger transition. In Fig. 7 we present the calculated and

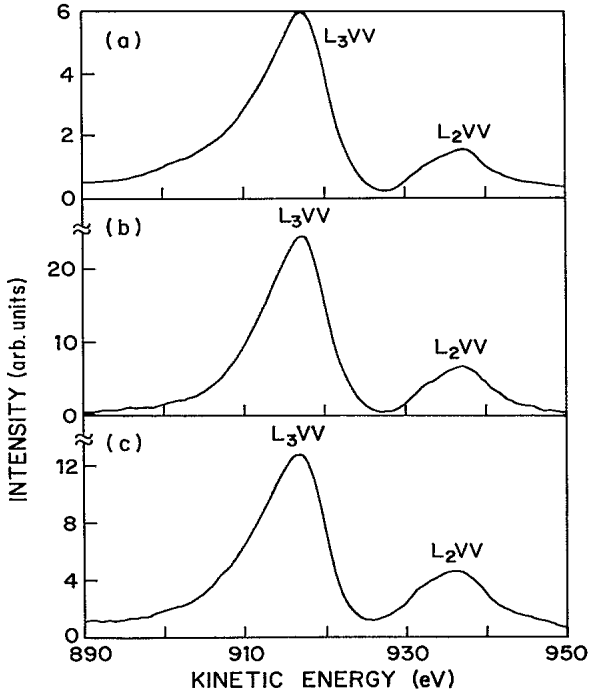

FIG. 5. Experimental Auger spectrum for copper in (a) $La_{1.85}Sr_{0.15}CuO_4$; (b) $La_{1.85}Ba_{0.15}CuO_4$; (c) $YBa_2Cu_3O_7$. The kinetic energy is relative to the Fermi level.

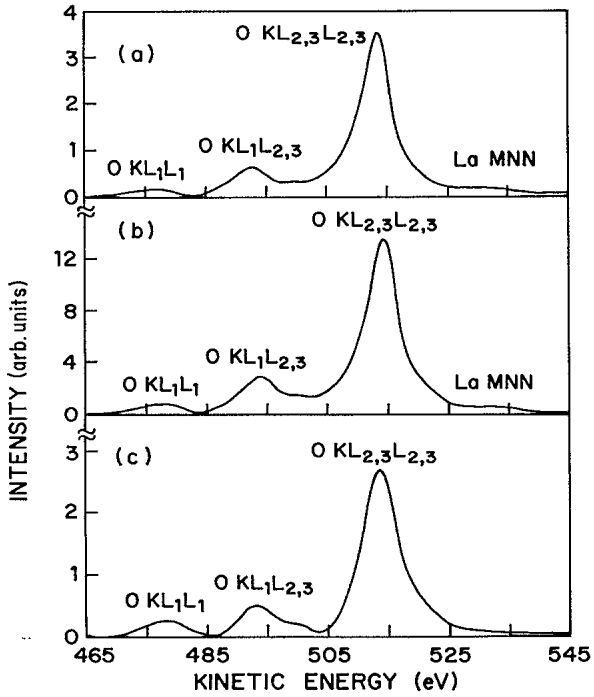

FIG. 6. Experimental Auger spectrum for oxygen in (a) $La_{1.85}Sr_{0.15}CuO_4$; (b) $La_{1.85}Ba_{0.15}CuO_4$; (c) $YBa_2Cu_3O_7$. The kinetic energy is relative to the Fermi level.

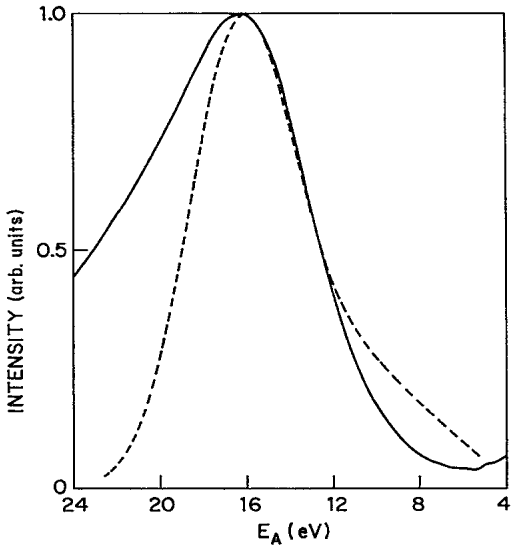

FIG. 7. Comparison between the experimental (solid) and calculated (dashed) Auger line shapes of the L_3VV transition of copper in $La_{1.85}Sr_{0.15}CuO_4$. E_A is the two-hole binding energy.

experimental Auger line shapes for copper in $La_{1.85}Sr_{0.15}CuO_4$. Similar results were obtained for copper in $La_{1.85}Ba_{0.15}CuO_4$. The values of U_d obtained by the above comparison are 7 ± 2 and 8 ± 2 eV for the Sr- and Ba-based La-Cu-O compounds, respectively. Balzarotti *et al.*[13] have calculated by a similar method the value of U_d in $YBa_2Cu_3O_7$ using the calculated results of Temmerman *et al.*[29] and obtained $U_d \sim 7$ eV. No detailed comparison of line shapes can be made, because the multiplet structure and the satellite structure due to the mixed valent (d^9-d^{10}) state of the copper ion were not considered.

A similar method is used for the oxygen atoms. As was mentioned above, oxygen atoms occupy two inequivalent crystallographic sites [O(1) and O(2)]. As a result there are differences in (1) the local density of states of the $2p$ valence bands, (2) the energy positions of the core states (chemical shifts), and (3) differences in the interaction parameter U. The band calculation resulted in two different PDOS's for the O(1) and O(2) atoms. They are to be related to the experimental Auger line shape, composed of the contributions of both types of oxygen atoms.

The numerical calculation of the Auger line shape consists of several steps. First, the calculation of the line shape using the expression (A4) for O(1) and O(2) was performed. A correct treatment involves the convolution of the p_x, p_y, and p_z PDOS's as explained in the Appendix. In the second step the interaction terms have to be included. The oxygen KL_3L_3 spectra consist of three components, one of which (the ^3P) is a forbidden transition which has negligible weight. The other two are the ^1G and the ^1S peaks, which have U's of $F^0+0.04F^2$ and $F^0+0.4F^2$, respectively.[30] As it is well established that the value of F^2, determining the multiplet splitting, is almost unchanged upon inserting atoms into a solid,[31] we use here $F^2=6.2$ eV, which is the value obtained from the ^1G-^1S splitting observed with optical spectroscopy of atomic oxygen.[32] F^0, on the other hand, depends strongly on the screening properties in the solid and may even be site dependent due to differences in local screening properties.

We used two independent values of F^0 for the two inequivalent oxygen sites in the fit to the experimental data. We still have to incorporate the O($1s$) core-level positions of the two types of oxygen. Experimentally no, or only a very small, difference in core-level binding energy has been observed between the two types of oxygen after clean sample surfaces were prepared.[3] On the other hand, a recent LMTO band-structure calculation for La_2CuO_4,[33] gives a rather large chemical shift of about 1.4 eV of the planar O($1s$) state towards higher binding energy relative to the apical oxygen. This is very close to the centroidal relative shift between the occupied O($2p$) levels.[33] In order to account for the above ambiguity in the relative positions of the core levels, we have repeated the calculations under two different assumptions. In one set of calculations we have put the O($1s$) threshold of both the apical and planar oxygen at 528 eV (corresponding to experiment). In the other set of calculations we have put the O($1s$) threshold of the apical oxygen O(2) at 528 eV (as before), but shifted the threshold of the planar oxygen O(1) to an energy which is higher by the centroidal relative shift between the occupied O($2p$) levels. This way both the $2p$ and the core levels supposedly correspond to the same calculation. In the last step we normalize and add the spectra of the two inequivalent oxygen atoms, and finally convolute the spectra with a Gaussian, as explained before for the copper atoms. An intrinsic lifetime broadening was taken into account by including an imaginary part in the denominators of Eqs. (1) and (A4). The parameters used in our fits are presented in Table IV.

In Fig. 8 we present the results of the fit together with the experimental data for the Sr-doped La-Cu-O compound [the same curve is obtained when the two above

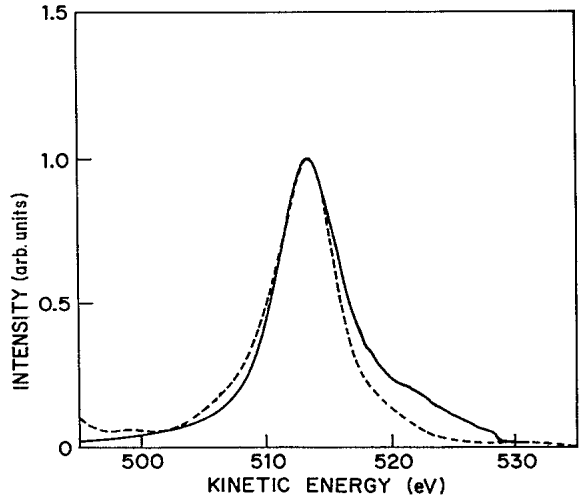

FIG. 8. Comparison between the experimental (dashed) and calculated (solid) Auger line shapes of the $KL_{2,3}L_{2,3}$ transition of oxygen in $La_{1.85}Sr_{0.15}CuO_4$.

TABLE IV. O(2p) centroids, and Coulomb parameters, in units of eV, used for fitting the oxygen KLL Auger spectra. Three different fits are presented here using (1) the present LMTO results for $La_{1.85}Sr_{0.15}CuO_4$ (La-Sr-Cu-O); (2) the present LMTO results for $La_{1.85}Ba_{0.15}CuO_4$ (La-Ba-Cu-O); (3) the centroids of the FLAPW results of Refs. 24 and 26 for La_2CuO_4. The binding energy of the O(1s) core level is either taken as 528 eV for both O(1) and O(2) (abbreviated by UC), or shifted for the O(1) atom to a value higher by the splitting between the O(1) and O(2) centroids (abbreviated by SC), as explained in the text. $U(^1G)$ and $U(^1S)$ are Slater integrals for the two multiplet components in the Auger spectra. The relative intensity of the ^1G peak is six times the ^1S intensity. We used the atomic value $F^2=6.2$ eV to calculate $U(^1G)$ and $U(^1S)$. Lifetime broadening of 2.5 eV and Gaussian broadening of 2.0 eV are used.

		Centroid	F^0	$U(^1G)$	$U(^1S)$
Present	O(1)(UC)	−5.7	3.0	3.2	5.5
LMTO	O(1)(SC)	−5.7	5.0	5.2	7.5
La-Sr-Cu-O	O(2)(UC)	−3.1	7.0	7.2	9.5
Present	O(1)(UC)	−5.3	2.5	2.7	5.0
LMTO	O(1)(SC)	−5.3	4.5	4.7	7.0
La-Ba-Cu-O	O(2)(UC)	−3.2	6.5	6.7	9.0
Refs. 24 and 26	O(1)(UC)	−3.9	5.1	5.3	7.6
FLAPW	O(1)(SC)	−3.9	6.2	6.4	8.7
La-Cu-O	O(2)(UC)	−2.8	7.3	7.5	9.8

assumptions for the position of the O(1) core level are used]. Similar results were obtained for the Ba-doped La-Cu-O compound. We see, that, although the line shape close to the main peak is in reasonable agreement, there is a significant discrepancy on the high-kinetic-energy side of the spectrum. The calculations give a much higher intensity here than the measured spectra. The high intensity in the calculations results from mixing of the quasiatomic two-hole bound state with the two-hole continuum on the high-kinetic-energy side. The latter continuum corresponds to having the holes on two different sites, where they do not interact, as expressed by the on-site interaction Hamiltonian leading to the Cini-Sawatzky expression. In our present LMTO calculations the single-hole continuum extends up to 9.5 eV, hence the two-hole continuum extends up to 19.0 eV. As a result the quasiatomic state is located near the edge of the two-hole continuum, resulting in strong mixing. Indeed, if the LMTO band-structure results of Ref. 33, which have narrower oxygen p bands, are used as our input, the calculated Auger spectrum has considerably less weight on the high-kinetic-energy side than the results shown in Fig. 8.

In order to check how our fits for the oxygen Coulomb parameters depend on the band-structure results that we use as an input, we have repeated the fit by replacing our centroidal relative shift between the occupied O(2p) levels by those obtained in the FLAPW calculation of Pickett *et al.*[24,26] for La_2CuO_4 (the latter centroids were obtained by digitizing the PDOS plots in Refs. 24 and 26, and have error bars of 0.5 eV due to uncertainties in the digitizing procedure). The result is presented together with our fits in Table IV.

An important conclusion from the fits presented in Table IV is that we need two different values of F^0, with the lower value corresponding to the planar oxygen O(1). This result is rather insensitive to the details of the fit, and is qualitatively the same for the two different band-structure calculations that we used (and also for an estimate based on Ref. 33), namely, it is unlikely to be due to inaccuracies in the band-structure calculation. It basically reflects the fact that the Auger spectrum has a single strong peak, whereas the centroids of the occupied PDOS's of the two oxygen sites differ by 1.1–2.6 eV, for the different band-structure results used for the fits (this difference is sufficient to split the peak in spite of the lifetime and Gaussian broadening used here). The splitting in F^0 halves when core-level shifts identical to the centroidal shifts are assumed, reflecting the fact that the PDOS represents a one-hole spectrum, while the Auger kinetic energy represents a two-hole spectrum. The shift in the centroids of the two-hole spectrum has to be compensated by a difference in U_p in order to get coinciding peak positions of the O(1) and O(2) contributions. A smaller value of U_p for the planar oxygen could reflect the fact that the screening in the CuO_2 planes is stronger. This is consistent with the notion that the conduction takes place in the planes.

On the basis of the different values of Coulomb parameters appearing in Table IV, we can conclude that U_p is approximately 5 and 7 eV on the O(1) and O(2) atoms, respectively, with error bars of about 2 eV. The direction of the splitting between them is, however, beyond the error bars, if our analysis is valid. AES evaluations of the intrasite oxygen U_p in Cu_2O have been made by Tjeng *et al.*,[34] who determined a value of $F^0=5.4\pm0.5$ eV. McMahan, Annett, and Martin[35] find by constrained-occupation LDA calculations on La_2CuO_4 F^0: 3.6 eV on O(1) and 3.0 eV on O(2). Thus they find smaller U_p values with an opposite anisotropy from ours.

V. DISCUSSION

It is rather surprising that, experimentally, a cancellation is found of the anisotropy both in the O(1s) XPS peak positions and the $K_1L_{2,3}L_{2,3}$ Auger lines (at least

within 0.5 eV of accuracy). It might, in principle, represent a surface preparation problem. If the surface structure is different from the bulk structure, and the oxygen atoms there are more equivalent than in the bulk, the splittings would tend to disappear. If this is the case, one cannot draw conclusions on splitting in the Coulomb parameter on the basis of the data observed here. However, many electron spectroscopy studies on different high-T_c cuprates prepared under proper experimental conditions (e.g., *in situ* scraping, fracturing, annealing) have shown that the main O(1*s*) core-level and Auger peaks are single.[3,36]

Alternatively one could suspect that the cancellation results form the particular set of band-structure calculations presented in this paper. However, the fact that calculations of three different groups (also of Ref. 33) give this anisotropy points to the possibility that the discrepancy is caused at a more profound level, e.g., due to the application of the LDA to this type of correlated electrons system. For such a system one expects self-energy corrections to become important, while they are treated only within a mean-field approximation in the single-particle PDOS's extracted from the LDA calculations.

A qualitative estimate of the effect of electron correlations on the above cancellation problem can be obtained on the basis of the approach of Zaanen, Sawatzky, and Allen[37] to the hybridization between oxygen bands and copper states treated in the quasiatomic limit. In this approach one finds for the Cu(3*d*) states a set of d^8 final states between 8 and 12 eV below E_F, and a d^{10} final state at about 1 eV above E_F instead of a single band (such as shown in Figs. 1–4). The effect of hybridization on the oxygen DOS is quite different now: The copper d^8 final states push the oxygen spectral weight towards and across E_F; the emptying of the states pushed across E_F corresponds to adding positive charge to the states near E_F, which in this case are mainly located at the planar O^{2-} ions, causing an increase of the core-level and 2*p* binding energies. In the LDA band scheme this positive charge has a considerably larger weight at the copper sites due to the larger hybridization. Therefore, in comparison with the LDA band calculation, the quasiatomic picture results in a shift of the O(2*p*) bands and core levels of the planar oxygen atoms toward higher binding energies, thereby reducing the anisotropy in core level and 2*p* band shifts between the two types of oxygen atoms. Thus the effect of electron correlations might reduce the anisotropy in U_p mentioned above.

VI. CONCLUSIONS

The on-site Coulomb parameters of the Cu(3*d*) and O(2*p*) states in $La_{1.85}Sr_{0.15}CuO_4$ and $La_{1.85}Ba_{0.15}CuO_4$ have been determined by comparing experimental Auger electron spectra and theoretical spectra based on LMTO band-structure calculations. We find O(2*p*) Coulomb parameters of approximately 5 and 7 eV for the planar and apical oxygen sites, respectively, and a Cu(3*d*) Coulomb parameter of 7–8 eV. The effect of electron correlations might reduce the anisotropy found in U_p.

ACKNOWLEDGMENTS

We would like to thank I. Felner for the samples used in the experiments and N. R. Armstrong for the deconvolution code of the inelastic-scattering contribution. One of us (D.v.d.M.) is indebted to G. A. Sawatzky for helpful discussions, and to the Max-Planck-Institut für Festkörperforschung, Stuttgart, Germany, for hospitality during part of this work. One of us (J.A.) acknowledges the hospitality of IRRMA, Federal Institute of Technology, Lausanne, Switzerland, during part of this work. This research was supported in part by the U.S.-Israel Binational Science Foundation.

APPENDIX

There are two inequivalent oxygen sites in tetragonal La_2CuO_4. One of them is the apical oxygen [O(2)], which is at a site with C_{4v} point-group symmetry having a bond to a neighboring oxygen atom in the *z* direction on one side only. The second type is the planar oxygen [O(1)] which is at a site of D_{2h} point-group symmetry. Note that this symmetry is also lower than the tetragonal symmetry due to strong covalent bonding in one planar direction and no covalent bonding in the other planar direction. There are two O(1) atoms per unit cell, one has its copper oxide bonds in the *x* direction, the other one in the *y* direction. As we will consider the ligand field splitting of the ^1D and the ^1S multiplets belonging to the $2p^4$ configuration in full rotational symmetry, the five-dimensional ^1D manifold ($|^1xy\rangle$, $|^1yz\rangle$, $|^1zx\rangle$, $(|^1xx\rangle-|^1yy\rangle)$, $(|^1xx\rangle+|^1yy\rangle+2|^1zz\rangle)$) splits up under C_{4v} into a two-dimensional manifold ($|^1yz\rangle$, $|^1zx\rangle$) and three one-dimensional manifolds, i.e., $|^1xy\rangle$, $(|^1xx\rangle-|^1yy\rangle)$, and $(|^1xx\rangle+|^1yy\rangle+2|^1zz\rangle)$. At the O(1) sites the degeneracy between $|^1zx\rangle$ and $|^1yz\rangle$ is lifted due to the absence of four-fold rotational symmetry. The single-particle DOS's are defined as

$$\rho_x(E)=\pi^{-1}\mathrm{Im}\left\langle x0\left|\frac{1}{E-H-i0^+}\right|x0\right\rangle , \tag{A1}$$

with similar expressions for $\rho_y(E)$ and $\rho_z(E)$. We adopt here a notation where the 0 in $|x0\rangle$ indicates the index of the site where the Auger process takes place. As for the present symmetries, *x*, *y*, and *z* are "good" quantum numbers and there are no matrix elements mixing $|x0\rangle$, $|y0\rangle$, and $|z0\rangle$. As a result the noninteracting two-particle Green's functions are diagonal on the basis $|^1xy\rangle$, $|^1yz\rangle$, $|^1zx\rangle$, $(|^1xx\rangle, |^1yy\rangle)$, $|^1zz\rangle$, where we adopted the abbreviated notation $|^1xy\rangle$ for $|^1x0,y0\rangle$, etc. It also follows from this that there are finite matrix elements connecting the $m_l=0$ states $|^1S^0\rangle$ and $|^1D^0\rangle$, which are $(|^1xx\rangle+|^1yy\rangle-|^1zz\rangle)$ and $(|^1xx\rangle+|^1yy\rangle+2|^1zz\rangle)$, respectively.

It is important to note that for the apical [O(2)] sites, the p_y PDOS and the p_x PDOS are equal. On the other hand, there is a large difference between these two PDOS's for the planar [O(1)] oxygen atoms, due to the difference in bonding in these two directions.

We are now ready to evaluate the site-projected

Green's functions necessary for the calculation of the Auger line profile. The Green's functions that we have to calculate are $G^{^1Di}_{^1Di}$, $G^{^1S}_{^1S}$, and $G^{^1S}_{^1D5}$. Here $|^1Di\rangle$ denotes the set $[(|^1xx\rangle-|^1yy\rangle)$, $|^1xy\rangle$, $|^1yz\rangle$, $|^1zx\rangle$, $(|^1xx\rangle+|^1yy\rangle+2|^1zz\rangle)]$ and $|^1S\rangle=(|^1xx\rangle+|^1yy\rangle-|^1zz\rangle)$. In the following equations we summarize the expressions for the unperturbed Green's functions, i.e., without electron-electron interactions:

$$
\begin{aligned}
g^{^1D1}_{^1D1} &= g^x_x \otimes g^y_y \ , \\
g^{^1D2}_{^1D2} &= g^y_y \otimes g^z_z \ , \\
g^{^1D3}_{^1D3} &= g^z_z \otimes g^x_x \ , \\
g^{^1D4}_{^1D4} &= \tfrac{1}{2}(g^x_x \otimes g^x_x + g^y_y \otimes g^y_y) \ , \\
g^{^1D5}_{^1D5} &= \tfrac{1}{6}(g^x_x \otimes g^x_x + g^y_y \otimes g^y_y + 4g^z_z \otimes g^z_z) \ , \\
g^{^1S}_{^1D5} &= (1/3\sqrt{2})(g^x_x \otimes g^x_x + g^y_y \otimes g^y_y - 2g^z_z \otimes g^z_z) \ , \\
g^{^1S}_{^1S} &= \tfrac{1}{3}(g^x_x \otimes g^x_x + g^y_y \otimes g^y_y + g^z_z \otimes g^z_z) \ .
\end{aligned}
\tag{A2}
$$

Here $\otimes$ indicates a convolution of the PDOS's. The site-projected Green's functions including interactions now follow from inverting the following Dyson equations:

$$
\begin{aligned}
G^{^1Di}_{^1Di} &= g^{^1Di}_{^1Di} + g^{^1Di}_{^1Di} U(^1D) G^{^1Di}_{^1Di} \quad (1 \le i \le 4) \ , \\
G^{^1S}_{^1S} &= g^{^1S}_{^1S} + g^{^1S}_{^1S} U(^1S) G^{^1S}_{^1S} + g^{^1D5}_{^1S} U(^1D) G^{^1S}_{^1D5} \ , \\
G^{^1D5}_{^1D5} &= g^{^1D5}_{^1D5} + g^{^1D5}_{^1D5} U(^1D) G^{^1D5}_{^1D5} + g^{^1S}_{^1D5} U(^1S) G^{^1D5}_{^1S} \ , \\
G^{^1D5}_{^1S} &= g^{^1D5}_{^1S} + g^{^1D5}_{^1S} U(^1D) G^{^1D5}_{^1D5} + g^{^1S}_{^1S} U(^1S) G^{^1D5}_{^1S} \ .
\end{aligned}
\tag{A3}
$$

The resulting expressions for the Green's functions, including electron-electron interactions at the site of the Auger process, are

$$
\begin{aligned}
G^{^1Di}_{^1Di} &= g^{^1Di}_{^1Di}[1 - g^{^1Di}_{^1Di} U(^1D)]^{-1} \quad (1 \le i \le 4) \ , \\
G^{^1S}_{^1S} &= D^{-1}[g^{^1S}_{^1S} - g^{^1D5}_{^1D5} U(^1D) g^{^1S}_{^1S} + g^{^1D5}_{^1S} U(^1D) g^{^1S}_{^1D5}] \ , \\
G^{^1D5}_{^1D5} &= D^{-1}[g^{^1D5}_{^1D5} - g^{^1S}_{^1S} U(^1S) g^{^1D5}_{^1D5} + g^{^1S}_{^1D5} U(^1S) g^{^1D5}_{^1S}] \ .
\end{aligned}
\tag{A4}
$$

$$
\begin{aligned}
G^{^1S}_{^1D5} &= D^{-1} g^{^1S}_{^1D5} \ , \\
D &\equiv [1 - g^{^1S}_{^1S} U(^1S)][1 - g^{^1D5}_{^1D5} U(^1D)] \\
&\quad - g^{^1D5}_{^1S} U(^1D) g^{^1S}_{^1D5} U(^1S) \ .
\end{aligned}
$$

[1] P. W. Anderson, Science **235**, 1196 (1987).

[2] L. F. Mattheiss, Phys. Rev. Lett. **58**, 1028 (1987); J. Yu, A. J. Freeman, and J.-H. Xu, *ibid.* **58**, 1035 (1987).

[3] K. C. Hass, in *Solid State Physics,* edited by H. Ehrenreich and D. Turnbull (Academic, New York, 1989), Vol. 42, p. 213; J. C. Fuggle, J. Fink, and N. Nücker, Int. J. Mod. Phys. B **2**, 1185S (1988).

[4] J. Ashkenazi and C. G. Kuper, in *Studies of High Temperature Superconductivity,* edited by A. Narlikar (Nova Science, Commack, NY, 1989), Vol. 3, p. 1; J. Genossar, B. Fisher, I. O. Lelong, J. Ashkenazi, and L. Patlagan, Physica C **157**, 320 (1989); J. Ashkenazi, in *Physical Phenomena at High Magnetic Fields,* edited by E. Manousakis *et al.* (Addison-Wesley, Reading, MA, 1991), p. 373.

[5] M. S. Hybertsen, M. Schlüter, and N. E. Christensen, Phys. Rev. B **39**, 9028 (1989).

[6] A. K. McMahan, J. F. Annett, and R. M. Martin, Phys. Rev. B **42**, 6268 (1990).

[7] R. S. List, A. J. Arko, Z. Fisk, S.-W. Cheong, S. D. Conradson, J. D. Thompson, C. B. Pierce, D. E. Peterson, R. J. Bartlett, N. D. Shinn, J. E. Schirber, B. W. Veal, A. P. Paulikas, and J. C. Campuzano, Phys. Rev. B **38**, 11 966 (1988); C. G. Olsen, R. Liu, A. B. Yang, D. W. Lynch, A. J. Arko, R. S. List, B. W. Veal, Y. C. Chang, P. Z. Jiang, and A. P. Paulikas, Science **245**, 731 (1989); J. C. Campuzano, G. Jennings, M. Faiz, L. Beaulaigue, B. W. Veal, J. Z. Liu, A. P. Paulikas, K. Vandervoort, H. Claus, R. S. List, A. J. Arko, and R. J. Bartlett, Phys. Rev. Lett. **64**, 2308 (1990).

[8] P. W. Anderson, in *High Temperature Superconductivity: Physical Properties, Electronic Structure and Mechanisms,* edited by J. Ashkenazi *et al.* (Plenum, New York, 1991); C. M. Varma, *ibid.*

[9] A. Fujimori, E. Takayama-Muromachi, Y. Uchida, and B. Okai, Phys. Rev. B **35**, 8814 (1987); P. Thiry, G. Rossi, Y. Petroff, A. Revcolevs, and J. Jegoudez, Europhys. Lett. **5**, 55 (1988).

[10] D. E. Ramaker, Appl. Surf. Sci. **21**, 2443 (1985).

[11] N. Nakayama, H. Fujita, T. Nogami, and Y. Shirota, Physica C **155**, 149 (1988).

[12] D. van der Marel, J. van Elp, G. A. Sawatzky, and D. Heitmann, Phys. Rev. B **37**, 5136 (1988).

[13] A. Balzarotti, M. De Crescenzi, N. Motta, F. Patella, and A. Sgarlata, Phys. Rev. B **38**, 6461 (1988); A. Balzarotti, in *Studied of High Temperature Superconductivity,* edited by A. Narlikar (Nova Science, Commack, NY, 1989), Vol. 4.

[14] M. Cini, Solid State Commun. **20**, 681 (1976); G. A. Sawatzky, Phys. Rev. Lett. **39**, 504 (1977).

[15] H. L. Skriver, *The LMTO Method: Muffin Tin Orbitals and Electronic Structure* (Springer-Verlag, New York, 1984).

[16] J. D. Jorgensen, H. B. Schüttler, D. G. Hinks, D. W. Capone II, K. Zhang, M. B. Brodsky, and D. J. Scalapino, Phys. Rev. Lett. **58**, 1024 (1987).

[17] M. Cini and C. Verdozzi, Nuovo Cimento **9**, 1 (1987).

[18] H. Eskes, L. H. Tjeng, and G. A. Sawatzky, Phys. Rev. B **41**, 288 (1990); H. Eskes and G. A. Sawatzky, *ibid.* **43**, 119 (1991).

[19] M. Vos, D. van der Marel, and G. A. Sawatzky, Phys. Rev. B **29**, 3073 (1984); M. Vos, G. A. Sawatzky, M. Davies, P. Weightman, and P. T. Andrews, Solid State Commun. **52**, 159 (1984).

[20] J. A. D. Matthew, M. Prutton, M. M. El Gomati, and D. C. Peacock, Surf. Interf. Anal. **11**, 173 (1988).

[21] M. C. Burrell and N. R. Armstrong, Appl. Surf. Sci. **17**, 53 (1977).

[22] K. Takegahara, H. Harima, and A. Yanase, Jpn. J. Appl. Phys. **26**, L352 (1987); D. A. Papaconstantopoulos, W. E. Pickett, and M. J. De Weert, Phys. Rev. Lett. **61**, 211 (1988); K. Schwarz, Solid State Commun. **64**, 421 (1987); D. W. Bullett and W. G. Dawson, J. Phys. C **20**, L853 (1987).

[23]G. M. Stocks, W. M. Temmerman, Z. Szotec, and P. A. Sterne, Supercond. Sci. Technol. **1**, 57 (1988).
[24]W. E. Pickett, H. Krakauer, D. A. Papaconstantopoulos, and L. L. Boyer, Phys. Rev. B **35**, 7252 (1987).
[25]W. M. Temmerman, G. M. Stocks, P. J. Durham, and P. A. Sterne, J. Phys. F **17**, L135 (1987); T. Oguchi, Jpn. J. Appl. Phys. **26**, L417 (1987).
[26]For a review, see W. E. Pickett, Rev. Mod. Phys. **61**, 433 (1989).
[27]N. Nücker, J. Fink, B. Renker, D. Ewert, and C. Politis, Z. Phys. B **67**, 9 (1987); J. C. Fuggle, P. J. W. Weijs, R. School, G. A. Sawatzky, J. Fink, N. Nücker, P. J. Durham, and W. M. Temmerman, Phys. Rev. B **37**, 123 (1988); P. Steiner, R. Courths, V. Kisinger, I. Sander, B. Siegwart, and S. Hüfner, Appl. Phys. A **44**, 75 (1987); B. Reihl, T. Riesterer, J. G. Bednorz, and K. A. Müller, Phys. Rev. B **35**, 8804 (1987); T. Takahashi, F. Maeda, S. Hosoya, and M. Sato, Jpn. J. Appl. Phys. **26**, L349 (1987); A. Fujimori, E. Takayama-Muromachi, Y. Uchida, and B. Okai, Phys. Rev. B **35**, 8814 (1987); P. Steiner, J. Albers, V. Kinsinger, I. Sander, B. Siegwart, S. Hüfner, and C. Politis, Z. Phys. B **66**, 275 (1987); N. T. Liang, K. H. Li, Y. C. Chou, M. F. Tai, and T. T. Chen, Solid State Commun. **64**, 761 (1987).
[28]D. D. Sarma and C. N. Rao, J. Phys. C **20**, L659 (1987); H. H. Madden, D. M. Zehner, and J. R. Noonan, Phys. Rev. B **17**, 3074 (1978); **18**, 2023 (1978); B. R. Chakravarty, D. D. Sarma, and C. N. Rao, Physica C **156**, 413 (1988); D. E. Ramaker, N. H. Turner, J. S. Murday, L. E. Toth, M. Osofsky, and F. L. Huston, Phys. Rev. B **56**, 5672 (1987); D. E. Ramaker, N. H. Turner, and F. L. Huston, *ibid.* **38**, 11 368 (1988); R. Bar-Deroma (Tyk), J. Felsteiner, R. Brener, and J. Ashkenazi, Physica C **162-164**, 1329 (1989).
[29]W. M. Temmerman, Z. Szotec, P. J. Durham, G. M. Stocks, and P. A. Sterne, J. Phys. F **17**, L319 (1987).
[30]J. C. Slater, *Quantum Theory of Atomic Structure* (McGraw-Hill, New York, 1960), Parts I & II.
[31]D. van der Marel and G. A. Sawatzky, Phys. Rev. B **37**, 10 674 (1988).
[32]C. E. Moore, *Atomic Energy Levels,* Natl. Bur. Stand. (U.S.) Circ. No. 467 (U.S. GPO, Washington, DC, 1958), Part I.
[33]O. Jepsen and O. K. Andersen (private communication); J. Zaanen, O. Jepsen, O. Gunnarsson, A. T. Paxton, O. K. Andersen, and A. Svane, Physica C **153-155**, 1636 (1988).
[34]L. H. Tjeng, J. van Elp, P. Kuiper, and G. A. Sawatzky (unpublished).
[35]A. K. McMahan, J. F. Annett, and R. M. Martin, Phys. Rev. B **42**, 6268 (1990).
[36]D. D. Sarma and A. Chainani, Phys. Rev. B **41**, 6688 (1990); D. E. Fowler, C. R. Brundle, J. Lerczak, and F. Holtzberg, J. Electron. Spectrosc. Relat. Phenom. **52**, 323 (1990).
[37]J. Zaanen, G. A. Sawatzky, and J. W. Allen, Phys. Rev. Lett. **55**, 418 (1985).